# Capacity of Steel-Concrete Composite Beams under Fire Conditions

**Abstract**

The behavior of structures under fire is quite complicated because of the high level ofnonlinearity at both element and material levels. With increasing the temperature, the material properties such as modules of elasticity decreases which makes the structure unable to support the applied loads. The structure members experience a thermal expansion during the fire which leads to significant restrained axial loads in these members which might lead to failure of the connection in steel structures. Also, steel structure might exhibits substantial creep at elevated temperature. On the other hand, the material properties of concrete such as compressive strength and elastic modulus deteriorate with high temperature as result, the connectors between the steel beam and the concrete slab might get affected. This study presents data and information about steel-concrete composite beams at ambient and high temperatures as well as the high temperature material properties of steel and concrete. Also, feasible way to protect steel section of composite beams by applying fire insulation with different thickness is discussed in this study.

## ١. Introduction

### ١،١ Steel-Concrete Composite beam at Ambient Temperature

In building and bridge structures, steel beams are frequently used to support concrete slabs. If there is an adequate connection to transfer longitudinal shear between the slab and the beam, then the two elements act together as a composite beam. The composite system consists of a steel beam, a concrete slab of some width and some kind of connector that transfers longitudinal shear between the beam and the slab, see Fig.(١).

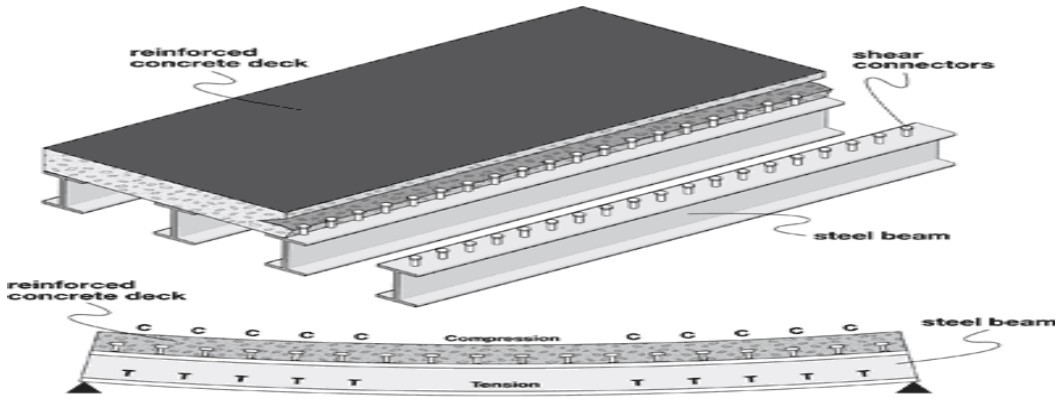


Fig. (١): Steel-Concrete Composite beam

The key to this added strength and stiffness is the increase moment of inertia of the composite cross section. This advantage is only true when the concrete is subject to compressive forces. Concrete is a brittle material whose tensile strength is quite variable and fractures (or cracks) with little or no warning. As a result, concrete is assumed to have no tensile strength and is ignored when it is in tension. On the other hand, concrete is very good in compression. This means that composite action is only of benefit in positive moment regions where concrete is on the compression side of the beam. In negative moment regions, where the concrete is on the tension side of beam, the concrete adds nothing to the strength or stiffness of the steel beam. Making use of composite behavior can significantly reduce the required size of a steel member, thus saving the extra cost associated with connecting the slab to the beam [١].

## ١.٢ Shear Strength of Composite Beam

The concrete does not contribute to the shear strength of the composite beam. The shear strength of composite beam will be determined based upon the properties of the steel section alone.

$V_u \leq \Phi V_n$

$V_n = ٠,٦F_yA_wC_v$

Where:

- $\Phi$ is reduction factor = ٠,٩
- $V_u$ is the maximum applied shear force.
- $٠,٦F_y$ is the shear yield strength of the steel.
- $A_w$ is the shear area of a web.
- $C_v$ is a modifier that accounts for buckling behavior of the web

## ١.٣ Moment Strength of Composite Beam

The nominal moment capacity, $M_n$, equals the internal couple formed by the tension and compression forces acting on the section below and above the plastic neutral axis.

$M_u \leq \Phi M_n$

$M_n$ = ($T_s$ or $C_c$) x (distance between $T_s$ and $C_c$)

$b_E = \min[L/٨,(\text{Overhang or } (C\text{-}C)/٢)]_{left} + \min[L/٨,(\text{Overhang or } (C\text{-}C)/٢)]_{right}$

Where:

- $\Phi$ is reduction factor = ٠,٩
- $M_u$ is maximum applied moment.
- $b_E$ is effective slab width.

Compute the moment strength of composite depend on the location of plastic neutral axis:

- The N.A locates in the beam web, see Fig.(٢).
- The N.A locates in the beam flange, see Fig.(٣).
- The N.A locates in the concrete slab, see Fig.(٤).

Under fire all previous questions and the following cases are valid taking in account the changing in neutral axes location and education of steel strength

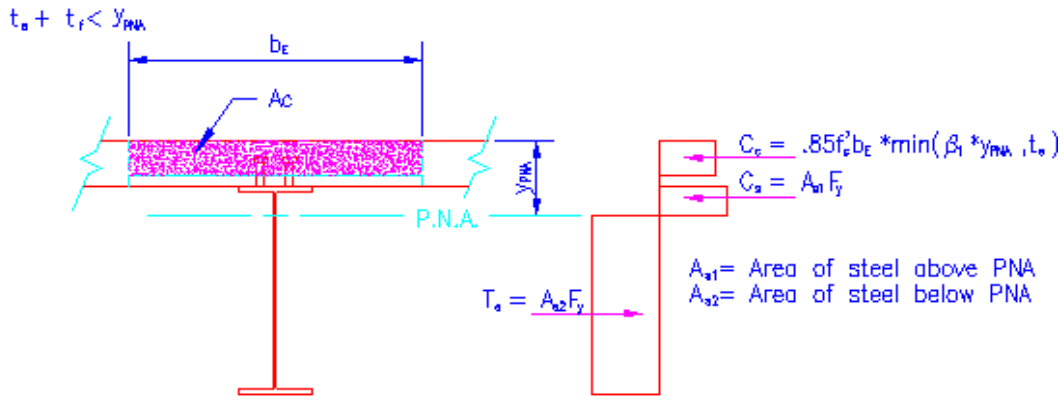


Fig. (٢): Neutral axis is in the beam web

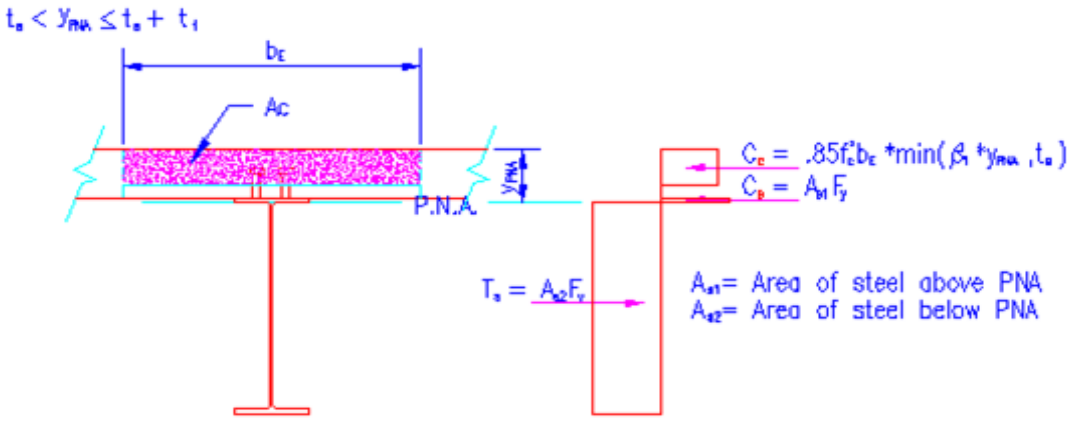


Fig. (٣): Neutral axis is in the beam flange

### ١.٤ Shear Connector Strength

Shear strength of the studs will depend on the transferred shear force that transferred between the beam and slab over a length from the location of maximum moment (where the internal forces are the greatest) and point of zero moment [١], see Fig.(٥).

$V' = S\ Q_n$

Where:

V' is the lesser value of the maximum of $T_s$ or $C_c$.

S is studs spacing.

$Q_n$ is the capacity of studs to transfer shear force and it is equal to the minimum of

(٠,٥ $A_{sc}$ sqrt ($f'_c$ $E_c$), $R_g R_p A_{sc} F_u$).

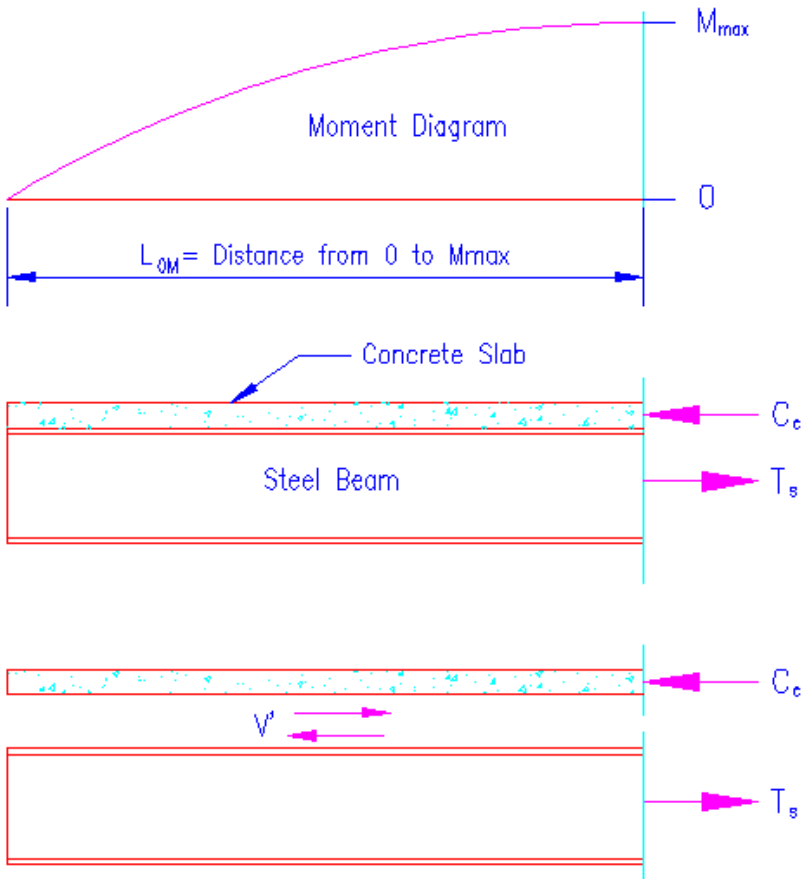


Fig. (٥): Free body diagram of partial beam

## ٢. Steel-Concrete Composite Beam at Elevated Temperature

The design equations that are used for composite beam at room temperature can be used at high temperature by considering the reduction factors for tensile strength (Fy) and modulus of elasticity (E) for steel and the compressive strength (fc) for concrete at the attending temperature during fire conditions. However, the behavior of composite beams under fire exposure can be more complicated than just considering these factors. This is due to complex phenomenon that occurs during fire such as axial restraint force that results from the thermal expansion of the steel which might affect the load carrying capacity of the composite beams. Also, the degree of the composition (shear studs) might be affected by the high temperature as well. The reduction factors for steel and concrete strength will be presented in next sections.

### ٢،١ State of Art of Composite Beams under Fire Conditions

Fakury [٢] presented a numerical analysis to verify if the simplified approach of the design of composite beams comprising steel beams with no encasement under fire that allowed by Eurocode ٤ would lead to appropriate design. Steel-concrete composite beam were used to find the temperature at the different points of the composite, see Fig. (٦). The Eurocode ٤ simplifications are :

١. For steel beams with contour encasement fire protection or unprotected, the bottom flange temperature can be determined as if it were subjected to fire on all four sides. For the top flange, the temperature can be assumed to be acting on three sides.
٢. For steel beams with contour encasement fire protection or unprotected, web temperature can be taken as the average between the temperature for the flange in case of sections with height equal or lower to ٤٠٠ mm. For higher height, web temperature can be taken as equal to the temperature at the bottom flange.
٣. Concrete slab temperature can be taken as ٤٠٪ of the upper flange in the calculation of the decrease of concrete strength for the design of shear connectors.
٤. The temperature of the shear connectors can be taken as ٨٠٪ of the temperature at the top flange.

It was found that:

١. Results for shear connecter temperature match the ٨٠٪of the temperature at the top of flange of the steel beam.
٢. Using of ٤٠٪ of the temperature at the top flange of the steel beam for concrete slab seems underestimate actual value calculation as ranging between ٥٠٪ and ٧٢٪.

٣. Average temperatures at concrete slab were similar to Eurocode ٤.

٤. At the bottom flange FEM temperature were ٣٪ to ٧٪ lower than Eurocode ٤.

٥. For the web, Eurocode ٤ results were up to ٢١٪ higher while for the top flange were ٤٤٪ to ٤٨٪ lower

٦. at the slab , temperature at the connectors were higher for Eurocode ٤ from ٠,٤٪ to ٣٢٪.

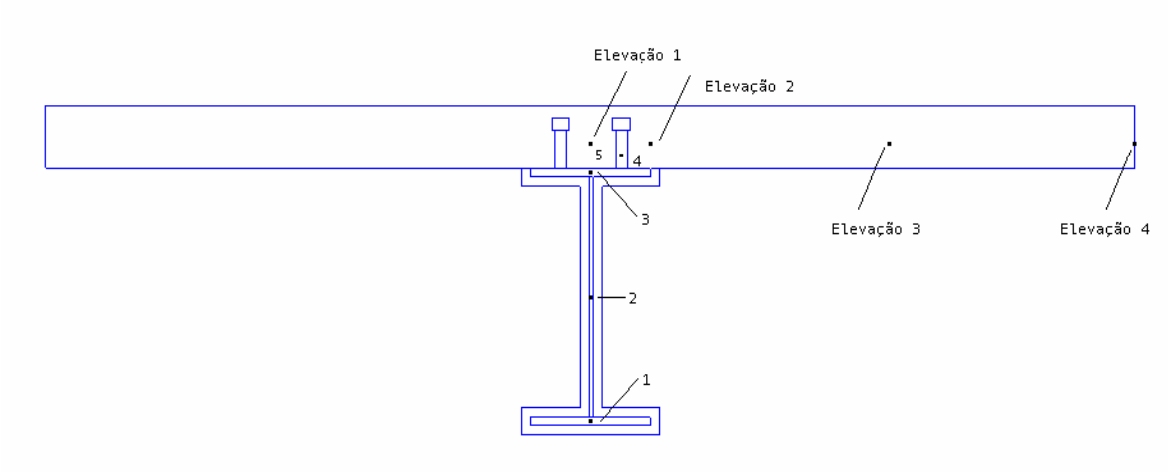


Fig. (٦): Location of thermocouple points

Wong [٣] developed a nonlinear finite element model to investigate the behavior of cellular composite beam at elevated temperature. For the concrete slab, a three dimensional eight- nodded solid element was used. Four – nodded quadrilateral shell elements were used to represent the cellular beam, see Fig.(٧). Slip between the concrete slab and steel beam was ignored. Both symmetric and asymmetric composite beams were analyzed. The Finite element results were compared with experimental work done by Nadjai. The finite element results show good agreement compare with the experimental results. All failure modes are accurately predicted by finite element model.

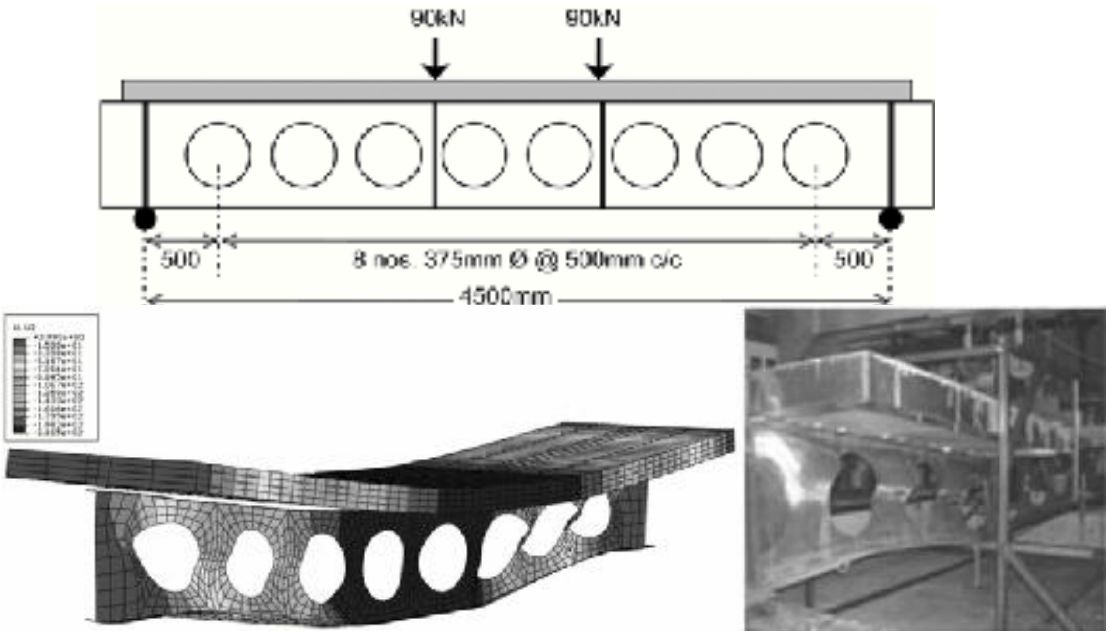


Fig. (٧): Cellular composite beam

Han [٤] carried a number of tests to investigate the fire performance of steel reinforced concrete beam to column joints. The beam –column joints were subjected to the ISO-٨٣٤ standard fire, see Fig. (٨). The tests were designed to investigate the effect of the load level in the reinforced concrete beam which is defined as a ratio of the longitudinal load to the beam bearing capacity at ambient temperature. Also, ABAQUS software was used in finite element analysis. Comparison of results calculated using the finite element modeling shows generally good agreement with the test result.

Fig. (٨): Concrete beam to column joint

Fabbrocino [٥] presented an experimental and analytical study on the behavior of composite steel-concrete beam subjected to negative bending. Three types of composite beams were used. The beam

type A is characterized by ٢٠ shear studs on a single row, uniformly distributed along the beam (spacing ١٩٠mm). The beam type B is characterized by ٢٠ shear studs, spaced ١٩٠mm, but concentrated at the ends on two rows while the beam type C has ٨ shear studs ٥١٥mm spaced, uniformly distributed along the beam, see Fig. (٩).

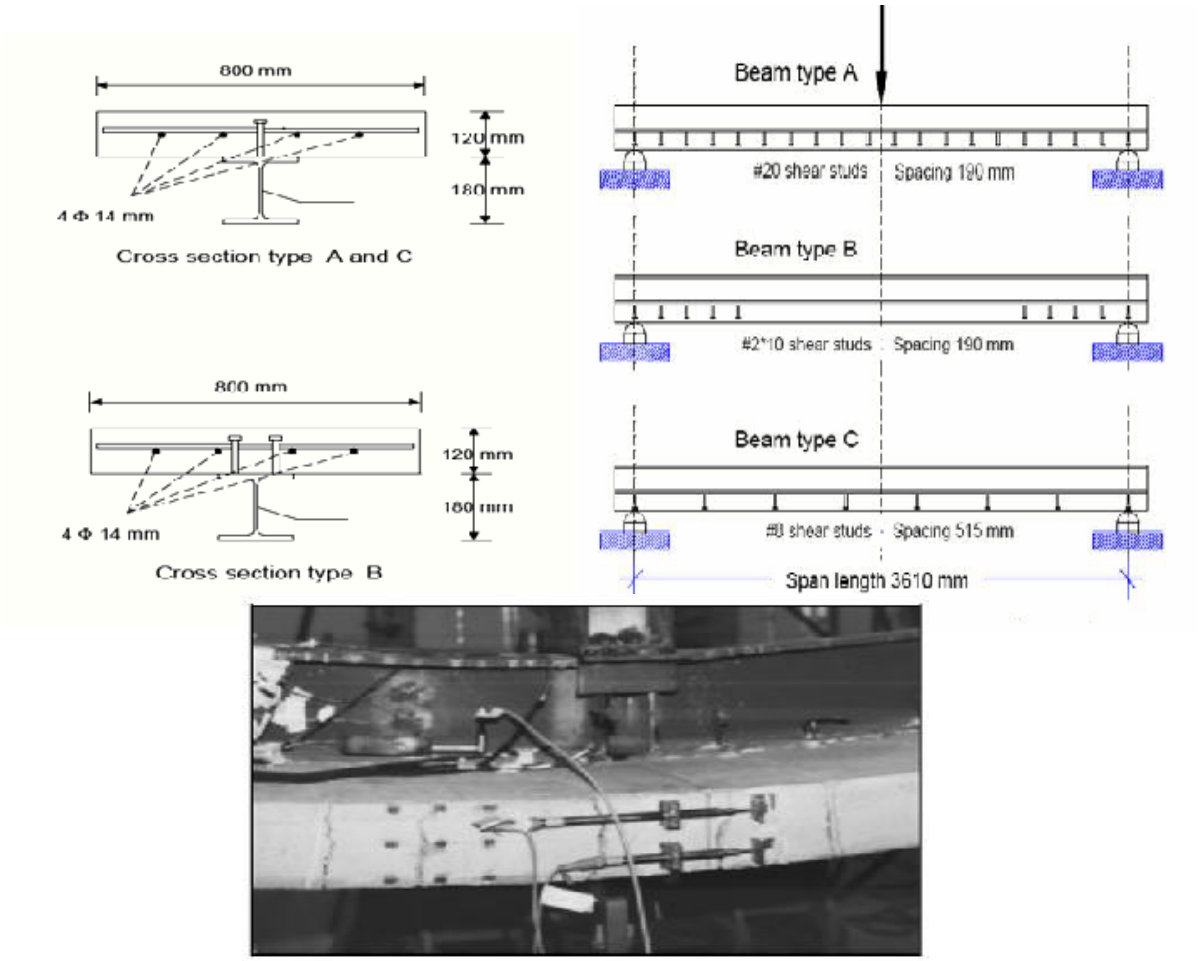


Fig. (٩): Experimental work cases

Korkess [٦] studied the behavior of composite steel- concrete beam subjected to negative bending using Ansys software in finite element analysis. Inverted composite beam subjected to concentrated load at the mid span were used to represent the negative bending. Elastic-plastic shell elements were used to modeling the steel section while solid element used for concrete slab, see Fig. (١٠). Nonlinear

springs were used to simulate the behavior of the shear connectors. Von Misses yield criteria with isotropic hardening rules were used to represent the steel beam. The reliability of the model is demonstrated by comparison with available experimental work which shows ٩٪-١٠٪ difference.

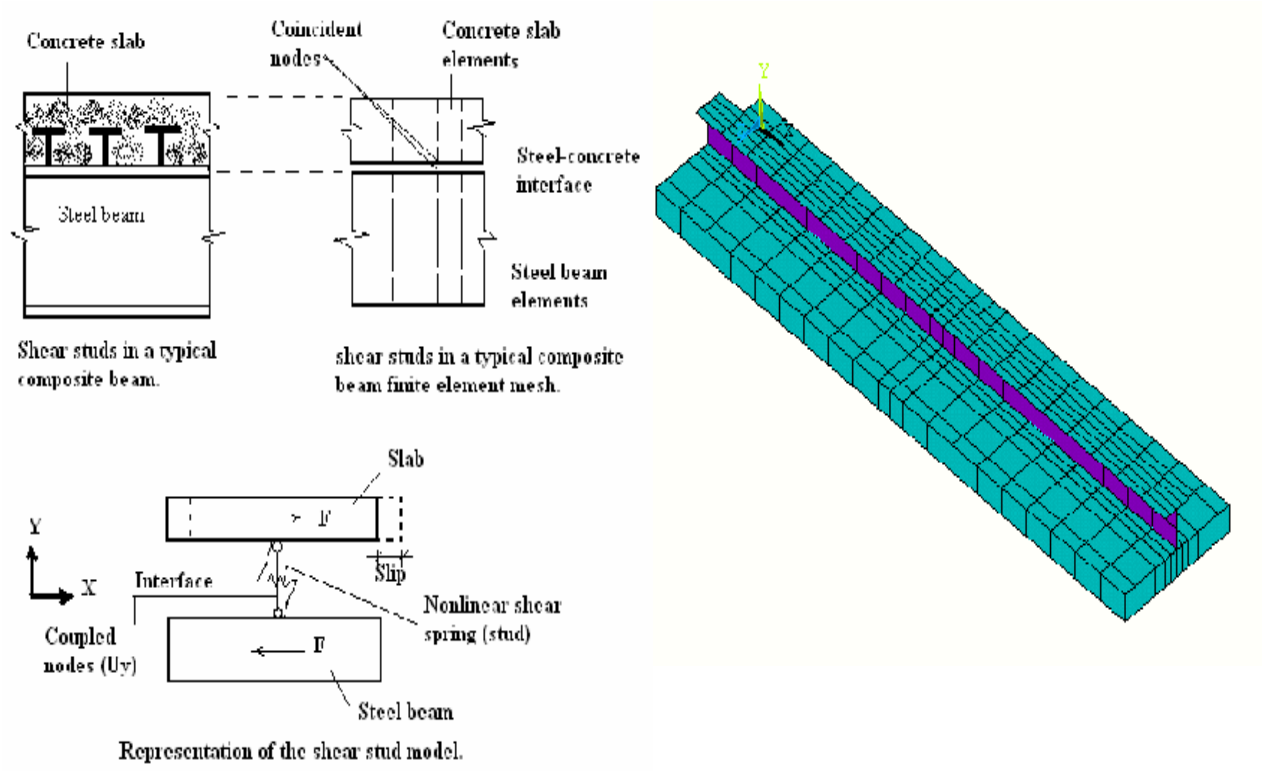


Fig. (١٠): Finite element simulation

## ٣. Material Properties of Steel at High-Temperature

### ٣.١ Stress Strain Relationship for Carbon Steel at Elevated Temperatures

A major problem of steel construction is that steel structural members have low fire resistance due high thermal conductivity and low specific heat of steel leading to faster reduction of strength with temperature [٧, ٨]. Also, at high temperature creep can be substantially high. Therefore, steel structural members can lose load carrying capacity at a rapid pace under elevated temperature [٩].

According to Eurocode ٣ [١٠] the following equation in Table (١) could be used to predict the stress strain relation for carbon steel at different temperatures. The stress-strain curve is shown in Fig. (١١), while the reduction of modulus of elasticity is considered as in Table (٢).

Table (١): Eurocode ٣ stress-strain relationship of steel at elevated temperatures

| Strain range | Stress $\sigma$ | Tangent modulus |
|---|---|---|
| $\varepsilon \le \varepsilon_{p,\theta}$ | $\varepsilon E_{a,\theta}$ | $E_{a,\theta}$ |
| $\varepsilon_{p,\theta} < \varepsilon < \varepsilon_{y,\theta}$ | $f_{p,\theta} - c + (b/a)\left[a^2 - (\varepsilon_{y,\theta} - \varepsilon)^2\right]^{0,5}$ | $\frac{b(\varepsilon_{y,\theta} - \varepsilon)}{a\left[a^2 - (\varepsilon_{y,\theta} - \varepsilon)^2\right]^{0,5}}$ |
| $\varepsilon_{y,\theta} \le \varepsilon \le \varepsilon_{t,\theta}$ | $f_{y,\theta}$ | 0 |
| $\varepsilon_{t,\theta} < \varepsilon < \varepsilon_{u,\theta}$ | $f_{y,\theta}\left[1 - (\varepsilon - \varepsilon_{t,\theta})/(\varepsilon_{u,\theta} - \varepsilon_{t,\theta})\right]$ | - |
| $\varepsilon = \varepsilon_{u,\theta}$ | 0,00 | - |
| Parameters | $\varepsilon_{p,\theta} = f_{p,\theta}/E_{a,\theta}$ $\varepsilon_{y,\theta} = 0,02$ | $\varepsilon_{t,\theta} = 0,15$ $\varepsilon_{u,\theta} = 0,20$ |
| Functions | $a^2 = (\varepsilon_{y,\theta} - \varepsilon_{p,\theta})(\varepsilon_{y,\theta} - \varepsilon_{p,\theta} + c/E_{a,\theta})$<br>$b^2 = c(\varepsilon_{y,\theta} - \varepsilon_{p,\theta})E_{a,\theta} + c^2$<br>$c = \frac{(f_{y,\theta} - f_{p,\theta})^2}{(\varepsilon_{y,\theta} - \varepsilon_{p,\theta})E_{a,\theta} - 2(f_{y,\theta} - f_{p,\theta})}$ | |

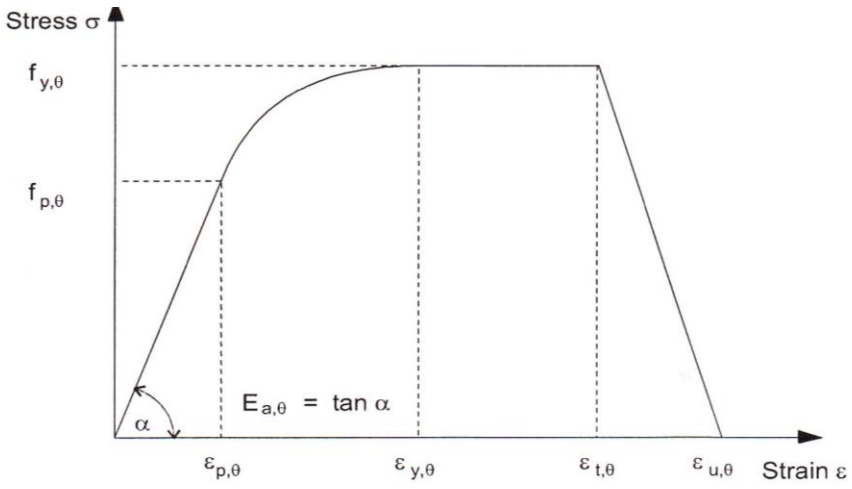


**Key:**

| | |
|---|---|
| $f_{y,\theta}$ | effective yield strength; |
| $f_{p,\theta}$ | proportional limit; |
| $E_{a,\theta}$ | slope of the linear elastic range; |
| $\varepsilon_{p,\theta}$ | strain at the proportional limit; |
| $\varepsilon_{y,\theta}$ | yield strain; |
| $\varepsilon_{t,\theta}$ | limiting strain for yield strength; |
| $\varepsilon_{u,\theta}$ | ultimate strain. |

Fig. (١١): Stress strain curve for carbon steel

Table (٢): Tensile strength and elastic modulus reduction factors for steel at elevated temperature

| Steel Temperature $\theta_a$ | Reduction factors at temperature $\theta_a$ relative to the value of $f_y$ or $E_a$ at 20°C | | |
|---|---|---|---|
| | Reduction factor (relative to $f_y$) for effective yield strength $k_{y,\theta} = f_{y,\theta}/f_y$ | Reduction factor (relative to $f_y$) for proportional limit $k_{p,\theta} = f_{p,\theta}/f_y$ | Reduction factor (relative to $E_a$) for the slope of the linear elastic range $k_{E,\theta} = E_{a,\theta}/E_a$ |
| 20°C | 1,000 | 1,000 | 1,000 |
| 100°C | 1,000 | 1,000 | 1,000 |
| 200°C | 1,000 | 0,807 | 0,900 |
| 300°C | 1,000 | 0,613 | 0,800 |
| 400°C | 1,000 | 0,420 | 0,700 |
| 500°C | 0,780 | 0,360 | 0,600 |
| 600°C | 0,470 | 0,180 | 0,310 |
| 700°C | 0,230 | 0,075 | 0,130 |
| 800°C | 0,110 | 0,050 | 0,090 |
| 900°C | 0,060 | 0,0375 | 0,0675 |
| 1000°C | 0,040 | 0,0250 | 0,0450 |
| 1100°C | 0,020 | 0,0125 | 0,0225 |
| 1200°C | 0,000 | 0,0000 | 0,0000 |

**NOTE:** For intermediate values of the steel temperature, linear interpolation may be used.

## ٣.٢ Thermal Elongation of Carbon Steels

The following equations could be used to determine the thermal strain of carbon steel at different temperatures [١٠], also see Fig. (١٢).

- for $20°C \leq \theta_a < 750°C$:

$$\Delta l/l = 1{,}2 \times 10^{-5}\,\theta_a + 0{,}4 \times 10^{-8}\,\theta_a^2 - 2{,}416 \times 10^{-4}$$

- for $750°C \leq \theta_a \leq 860°C$:

$$\Delta l/l = 1{,}1 \times 10^{-2}$$

- for $860°C < \theta_a \leq 1200°C$:

$$\Delta l/l = 2 \times 10^{-5}\,\theta_a - 6{,}2 \times 10^{-3}$$

where:

| | | |
|---|---|---|
| $l$ | is | the length at 20°C; |
| $\Delta l$ | is | the temperature induced elongation; |
| $\theta_a$ | is | the steel temperature [°C]. |

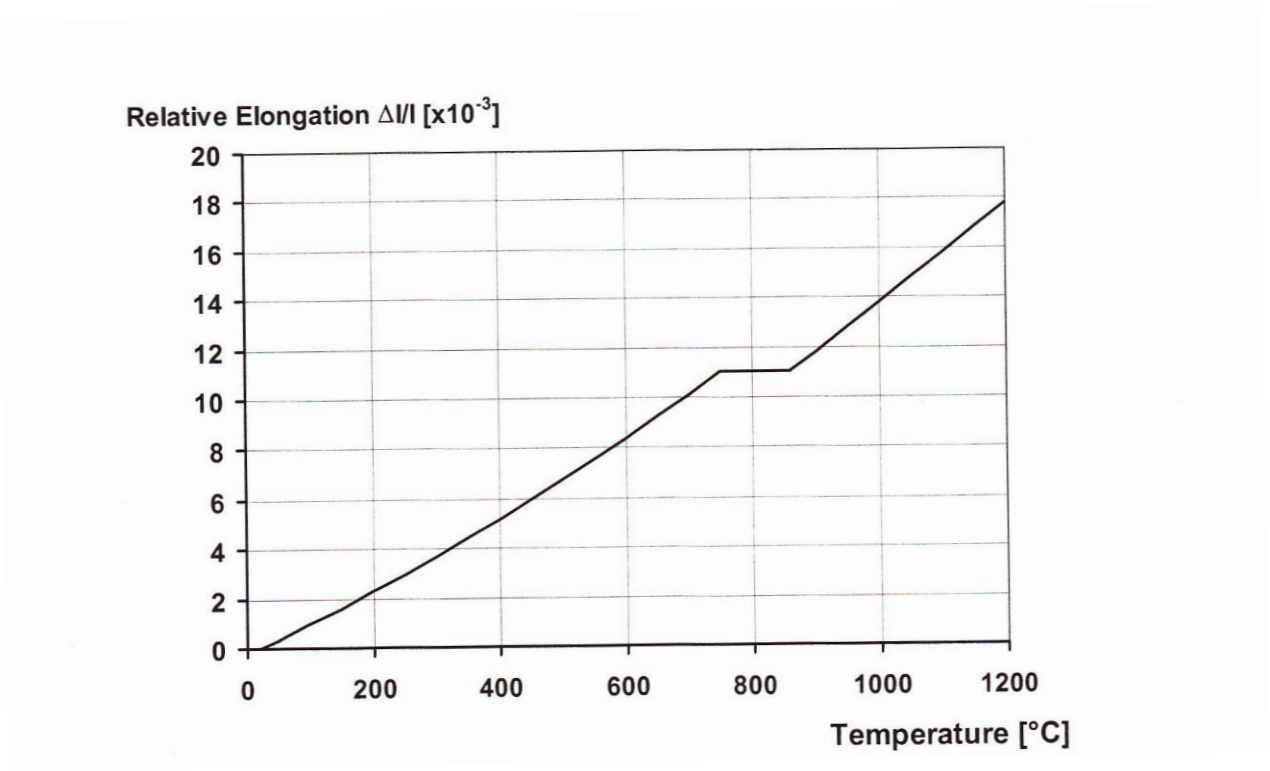


Fig.(١٢) Thermal strain of steel

## ٤. Material Properties of Concrete at High-Temperature

### ٤.١ Stress Strain Relationship for Concrete at Elevated Temperatures

According to Eurocode ٢ [١١] the following equation in Table (٣) can be used to predict the stress strain relation for concrete at different temperatures. The stress-strain curve is shown in Fig. (١٣), while the reduction of compressive strength is considered as in Table (٤).

Table (٣): Eurocode ٢ stress-strain relationship of concrete at elevated temperatures

| Range | Stress $\sigma(\theta)$ |
|---|---|
| $\varepsilon \leq \varepsilon_{c1,\theta}$ | $\frac{3\varepsilon f_{c,\theta}}{\varepsilon_{c1,\theta}\left(2+\left(\frac{\varepsilon}{\varepsilon_{c1,\theta}}\right)^3\right)}$ |
| $\varepsilon_{c1(\theta)} < \varepsilon \leq \varepsilon_{cu1,\theta}$ | For numerical purposes a descending branch should be adopted. Linear or non-linear models are permitted. |

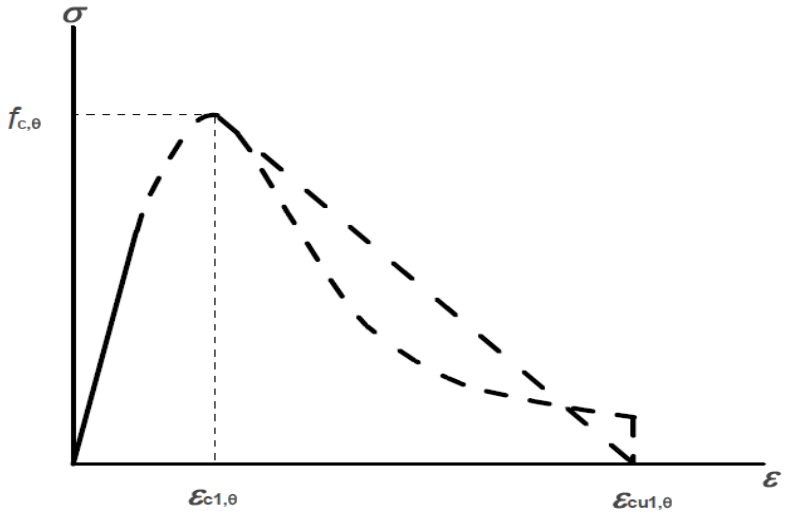


Fig. (١٣): Stress strain curve for concrete

Table (٤): Compressive strength reduction factors for concrete at elevated temperature

| Concrete temp. $\theta$ | Siliceous aggregates | | | Calcareous aggregates | | |
|---|---|---|---|---|---|---|
| | $f_{c,\theta} / f_{ck}$ | $\varepsilon_{c1,\theta}$ | $\varepsilon_{cu1,\theta}$ | $f_{c,\theta} / f_{ck}$ | $\varepsilon_{c1,\theta}$ | $\varepsilon_{cu1,\theta}$ |
| [°C] | [-] | [-] | [-] | [-] | [-] | [-] |
| 1 | 2 | 3 | 4 | 5 | 6 | 7 |
| 20 | 1,00 | 0,0025 | 0,0200 | 1,00 | 0,0025 | 0,0200 |
| 100 | 1,00 | 0,0040 | 0,0225 | 1,00 | 0,0040 | 0,0225 |
| 200 | 0,95 | 0,0055 | 0,0250 | 0,97 | 0,0055 | 0,0250 |
| 300 | 0,85 | 0,0070 | 0,0275 | 0,91 | 0,0070 | 0,0275 |
| 400 | 0,75 | 0,0100 | 0,0300 | 0,85 | 0,0100 | 0,0300 |
| 500 | 0,60 | 0,0150 | 0,0325 | 0,74 | 0,0150 | 0,0325 |
| 600 | 0,45 | 0,0250 | 0,0350 | 0,60 | 0,0250 | 0,0350 |
| 700 | 0,30 | 0,0250 | 0,0375 | 0,43 | 0,0250 | 0,0375 |
| 800 | 0,15 | 0,0250 | 0,0400 | 0,27 | 0,0250 | 0,0400 |
| 900 | 0,08 | 0,0250 | 0,0425 | 0,15 | 0,0250 | 0,0425 |
| 1000 | 0,04 | 0,0250 | 0,0450 | 0,06 | 0,0250 | 0,0450 |
| 1100 | 0,01 | 0,0250 | 0,0475 | 0,02 | 0,0250 | 0,0475 |
| 1200 | 0,00 | - | - | 0,00 | - | - |

### ٤.٢ Thermal Elongation of Carbon Steels

The following curves in Fig. (١٤) can be used to determine the thermal strain of concrete at different temperatures [١١].

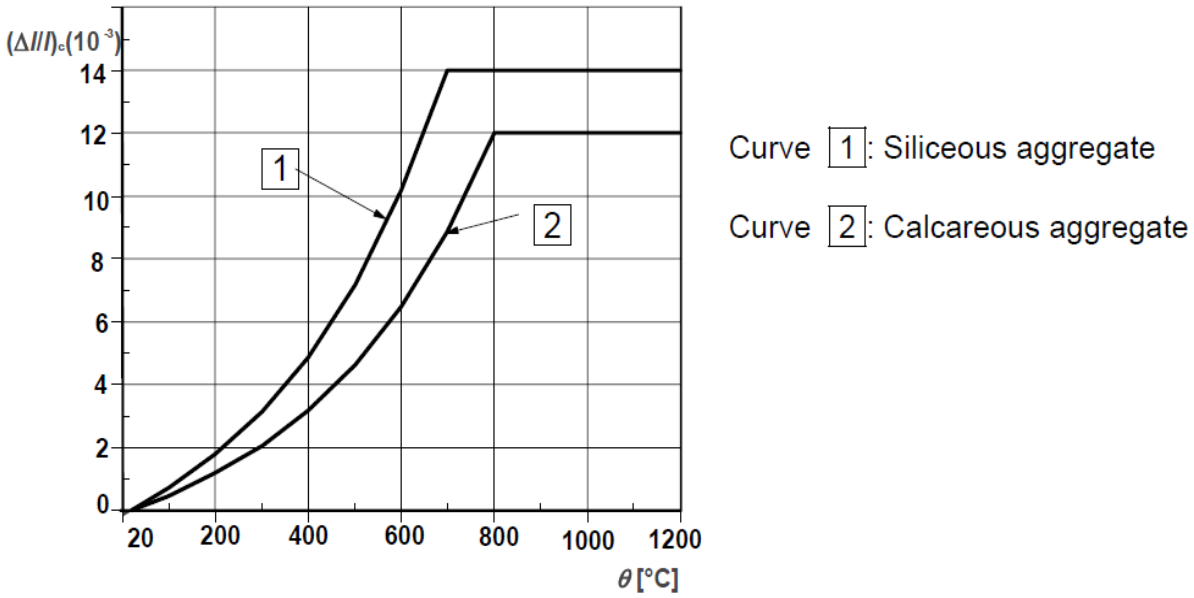


Fig. (١٤): Thermal elongation of concrete at elevated temperatures

### ٥. Fire Protection of Composite beams

In many cases fire in building gets extinguished by firefighter and the structural members exposed to fire might retain most its capacity. Results from previous research showed that steel-concrete composite girders can retain about ٧٠-٨٠٪ of its capacity when it's exposed to maximum temperature of ٦٠٠ °C [١٢]. This is due to residual strength of steel that regain most of its tensile strength when it is heated to temperature of ٦٠٠°C the cool down to room temperature [١٣]. On the other hand, similar structural members can experience failure when exposed to temperature around ١٠٠٠ °C [١٤]. Therefore in conditions of intense fire exposure conditions, structural members need to be protected from fire. One of the effective to insulate the steel section of the composite beam by applying fire insulation material that has less conductivity and higher specific heat. These insulation materials can be applied with thickness of ١٢ mm or ٢٥ mm to provide the ٢ or hours fire resistance for these members [١٥, ١٦].

## ٦. Conclusions

From the information presented in this study about the steel-concrete composite beam capacity about room and elevated temperature, the following conclusion can be made:

- Fire can have a significant effect on the load carrying capacity of composite beams
- The capacity of composite beams at elevated temperature depends on the temperature attend during fire exposure.
- The capacity of composite beams at elevated temperature reduces based on the reduction of steel and concrete strength.
- To calculate the capacity of composite beams, equation similar to the room temperature capacity can be used taking in count the reduction factor of steel and concrete due to fire condition.
- The tensile strength of steel reduces by ٥٠٪ and the elastic modulus by ٧٠٪ at temperature of ٦٠٠ °C.
- The compressive strength of concrete reduces by ٥٥٪ when high temperature of concrete reaches ٦٠٠ °C.
- The composite beam can be protected from fire effect by applying different thickness of fire insulation on the steel section while the concrete slabs don’t need any protections.

## ٧. References


١. T. Bartlett Quimby (٢٠٠٨), “A Beginners Guides to Steel Construction Manual”.

٢. Ricardo H. Fakury , Estevam B. Las Casas , Fernando P. F. J nior , and Laura M. P. Abreu (٢٠٠٢). “ Numerical Analysis of the Eurocode Assumptions for Temperature Distribution in Composite Steel and Concrete Beams”.

٣. Vuiyee Bernice Wong, Ian Burgess, and Roger Plank (٢٠٠٩). “Behaviour of Composite Cellular Steel - Concrete Beams at Elevated Temperatures”. Steel Structure,

٤. Lin-Hai Han , Yong-Qian Zheng, Zhong Tao (٢٠٠٤) “Fire Performance of Steel Reinforced Concrete (SRC) Beam-to-Column joints”.

٥. R.H. Fakury ,E.B.LasCasas,F.Pac ficoF.Jr.,L.M.P.Abreu (٢٠٠٥) “Design of Semi-Continuous Composite Steel–Concrete Beams at the Fire Limit State”. Journal of Constructional Steel Research.

٦. Ikbal N.Korkess, Anas H. Yousifany, Dr.Qais Abdul-Majeed, and Husain M. Husain (٢٠٠٩).” Behavior of Composite Steel-Concrete Beam Subjected to Negative Bending”. Eng.& Tech. Journal ,Vol.٢٧, No.١.

٧. Esam M. Aziz, Venkatesh K. Kodur, Jonathan D. Glassman, Maria E. Moreyra Garlock (٢٠١٥) "Behavior of Steel Bridge Girders under Fire Conditions" Journal of Constructional Steel Research, vol. ١٠٦: pp. ١١-٢٢.

٨. Venkatesh K. Kodur, Esam M. Aziz, Mahmud M. Dwaikat (٢٠١٣) "Evaluating Fire Resistance of Steel Girders in Bridges" ASCE/Journal of Bridge Engineering, vol. ١٨ (٧): pp. ٦٣٣-٦٤٣.

٩. Venkatesh K. Kodur, Esam M. Aziz (٢٠١٤) "Effect of Temperature on Creep in ASTM A٥٧٢ High-Strength Low-Alloy Steels" Journal of Materials and Structures, vol. ٤٨(٦): pp. ١٦٦٩-١٦٧٧.

١٠. BS,EN ١٩٩٣-١-٢ , Eurocode ٣ (٢٠٠٥), “Design of Steel Structure, part ١-٢: General Rules- Structural Fire Desigen”. The European Standard.

١١. BS,EN ١٩٩٣-١-٢ , Eurocode ٢ (٢٠٠٥), “Design of Concrete Structure, part ١-٢: General Rules- Structural Fire Desigen”. The European Standard.

١٢. Esam M. Aziz, Venkatesh K. Kodur (٢٠١٣) "An Approach for Evaluating the Residual Strength of Fire Exposed Bridge Girders" Journal of Constructional Steel Research, vol. ٨٨: pp. ٣٤-٤٢.

١٣. Esam M. Aziz, Venkatesh Kodur (٢٠١٥) “Effect of Temperature and Cooling Regime on Mechanical Properties of High-Strength Low-Alloy Steel” Journal of Fire and Materials, vol. ٤٠ (٧): pp. ٩٢٦-٩٣٩.

١٤. Jonathan D. Glassman, Maria E. Moreyra Garlock, Esam M. Aziz, Venkatesh K. Kodur (٢٠١٦) “Modeling Parameters for Predicting the Ultimate Postbuckling Shear Strength of Steel Plate Girders” Journal of Constructional Steel Research, vol. ١٢١: pp. ١٣٦-١٤٣.

١٥. Venkatesh K. Kodur, Esam M. Aziz, Mohannad Z. Naser (٢٠١٦) “Strategies for Enhancing Fire Performance of Steel Bridges" Journal of Engineering Structures, vol. ١٣١: pp. ٤٤٦-٤٥٨.

١٦. Esam M. Aziz (٢٠١٧) “Enhancing Fire Resistance of Steel Bridge Girders using External Fire Insulation” Kurdistan Journal of Applied Research, vol. ٢: pp. ٣١٥-٣١٩.